

Spatial charting of single cell transcriptomes in tissues

Wei and He et al.

Supplementary Materials

CONTENTS

Supplementary Figure 1

Overview of two downstream computational modules of the CellTrek toolkit.....Page 3

Supplementary Figure 2

Three spatial single-cell datasets for benchmarking.....Page 4

Supplementary Figure 3

Benchmarking on three datasets with known spatial references.....Page 5

Supplementary Figure 4

Simulation study of CellTrek under different data conditions.....Page 7

Supplementary Figure 5

Mouse brain and kidney co-expression module enrichment analysis and mouse kidney spatial constrained cell-cell interaction analysis.....Page 9

Supplementary Figure 6

CellTrek analysis of mouse hippocampus Slide-seq data.....Page 11

Supplementary Figure 7

ScRNA-seq and ST analyses of DCIS1.....Page 12

Supplementary Figure 8

Spatial co-expression patterns of tumor cells in DCIS1.....Page 13

Supplementary Figure 9

ScRNA-seq data analysis of DCIS2.....Page 15

Supplementary Figure 10

CellTrek analyses of myeloid cell states in DCIS2.....Page 16

Supplementary Figure 11

Orthogonal validation of tumor and immune cell spatial distributions using RNAscope assay in DCIS2 and DCIS3.....Page 17

Supplementary Table 1

Parameter settings for different conditions in simulation-1.....Page 19

Supplementary Table 2

Parameter settings for different conditions in simulation-2.....Page 20

Supplementary Table 3

Parameter settings for different marker points in simulation-3.....Page 21

Supplementary Data 1

Screenshot of the CellTrek result for mouse brain data.....Page 22

Supplementary Data 2

Screenshot of the CellTrek result for mouse kidney data.....Page 23

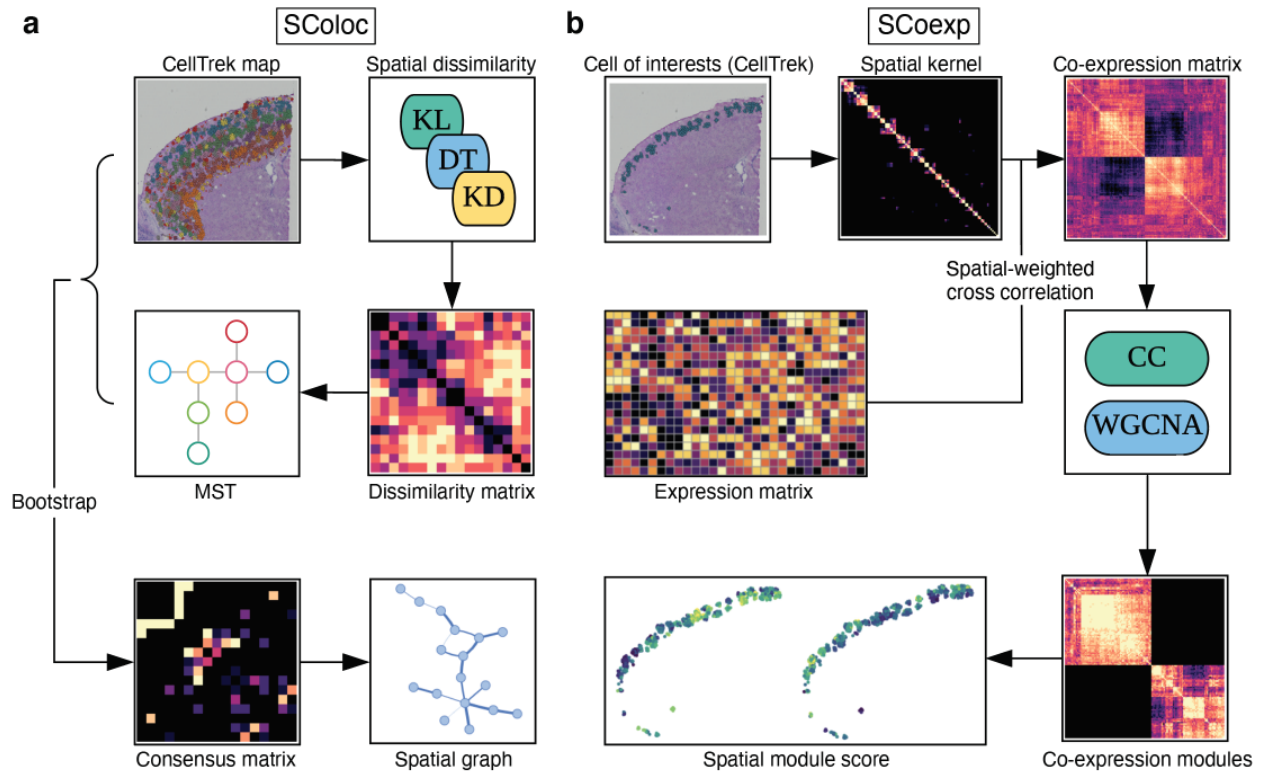
Supplementary Data 3

Screenshot of the CellTrek result for DCIS1 data.....Page 24

Supplementary Data 4

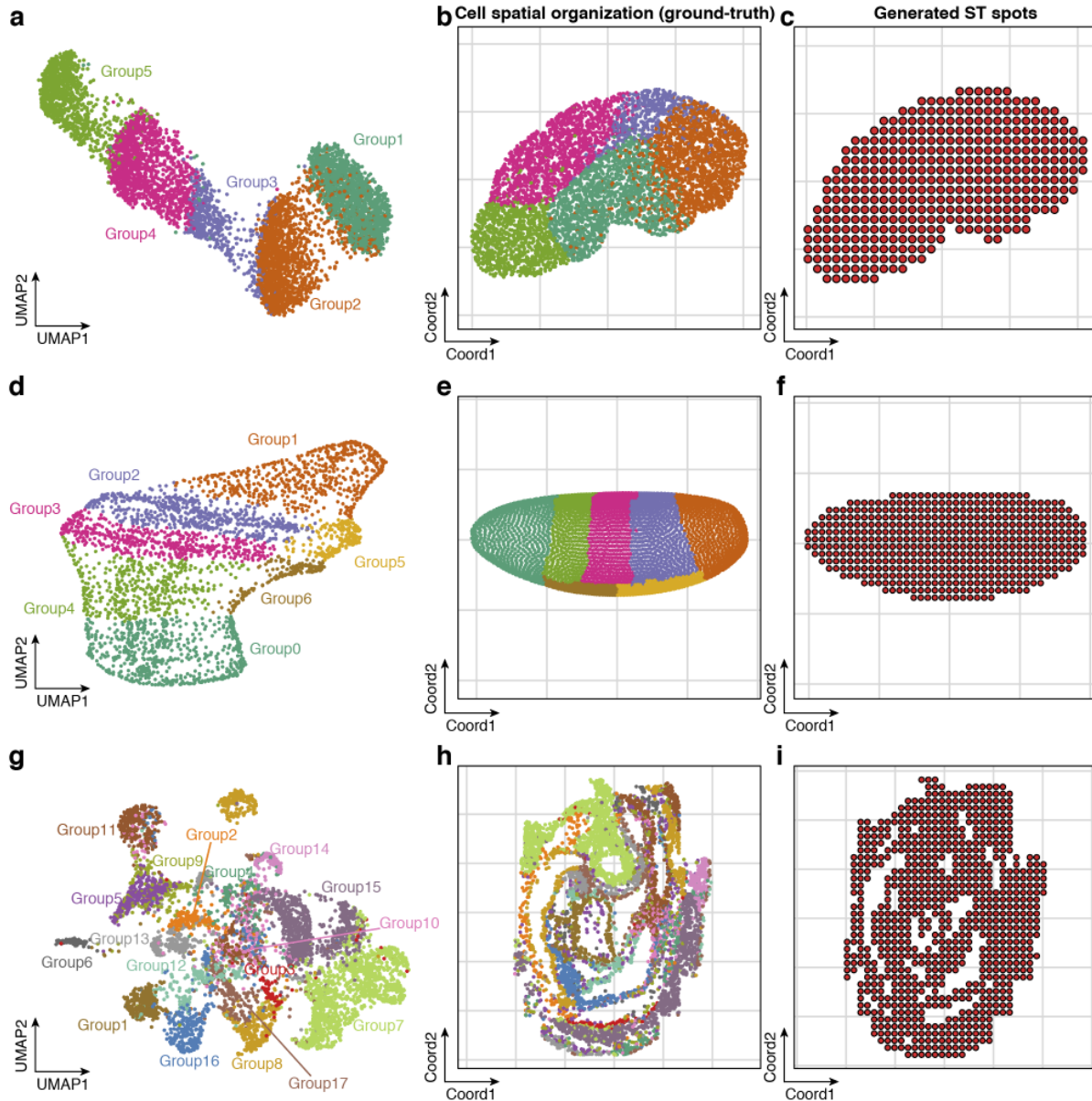
Screenshot of the CellTrek result for DCIS2 data.....Page 25

Supplementary Figures



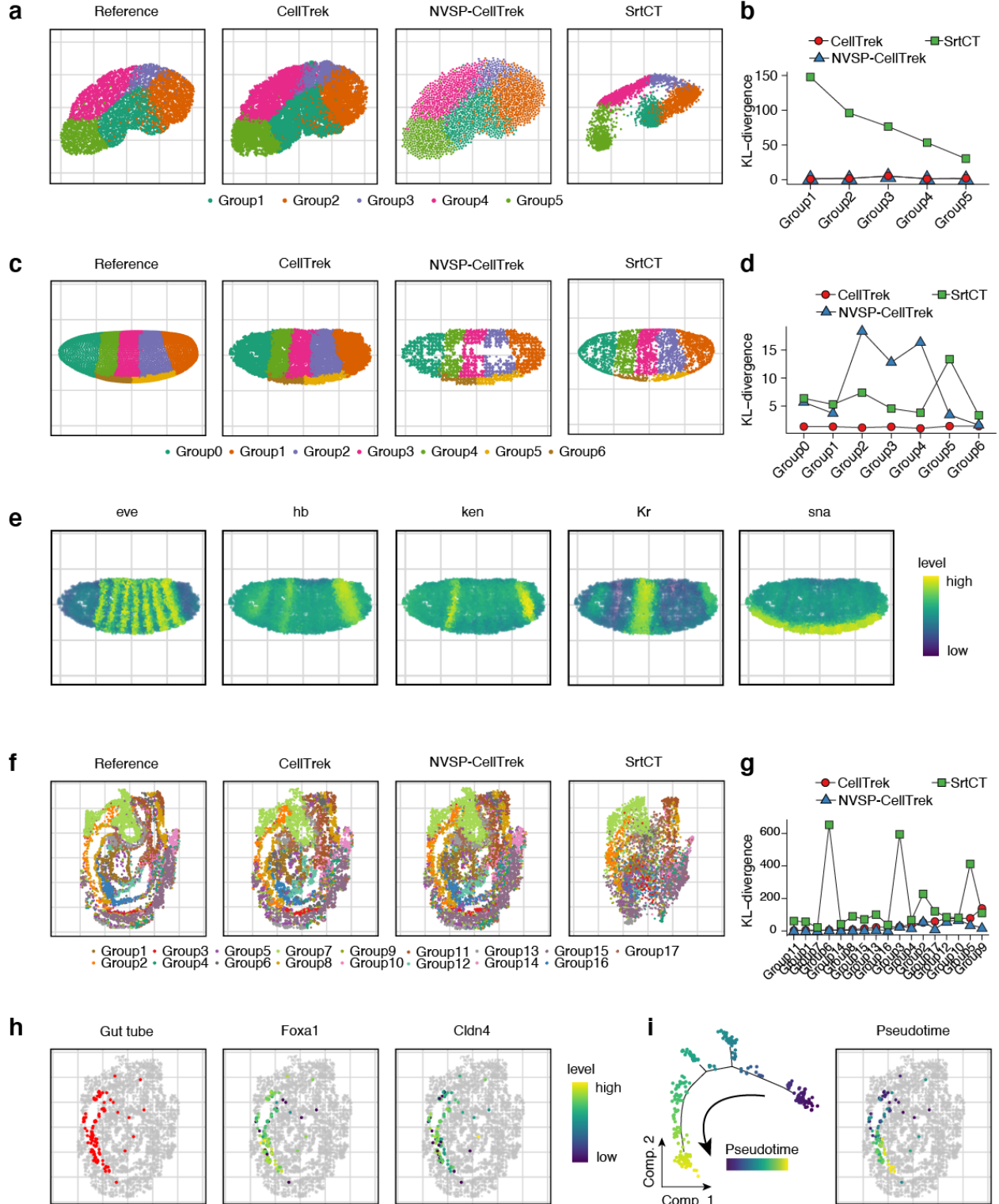
Supplementary Figure 1 – Overview of two downstream computational modules of the CellTrek toolkit

(a) The SColoc module. Based on the CellTrek result map, three different spatial dissimilarity methods, i.e., KL, DT, KD, can be applied to calculate a cell-type spatial dissimilarity matrix, and an MST is used to generate a tree structure. These steps are conducted repetitively on bootstrapped samples to calculate a consensus matrix on dissimilarity matrices or MSTs, which produces a final cell-type spatial graph representation. (b) The SCoexp module. For cells of interest, based on the CellTrek map, SCoexp first calculates a spatial kernel matrix using RBF based on their spatial distance. Next, based on the spatial kernel matrix and cell-gene expression matrix, SCoexp calculates the spatial weighted gene co-expression. Gene modules are then identified using CC or WGCNA. For the identified co-expression modules, module activity scores can be computed and mapped back to the CellTrek coordinates.



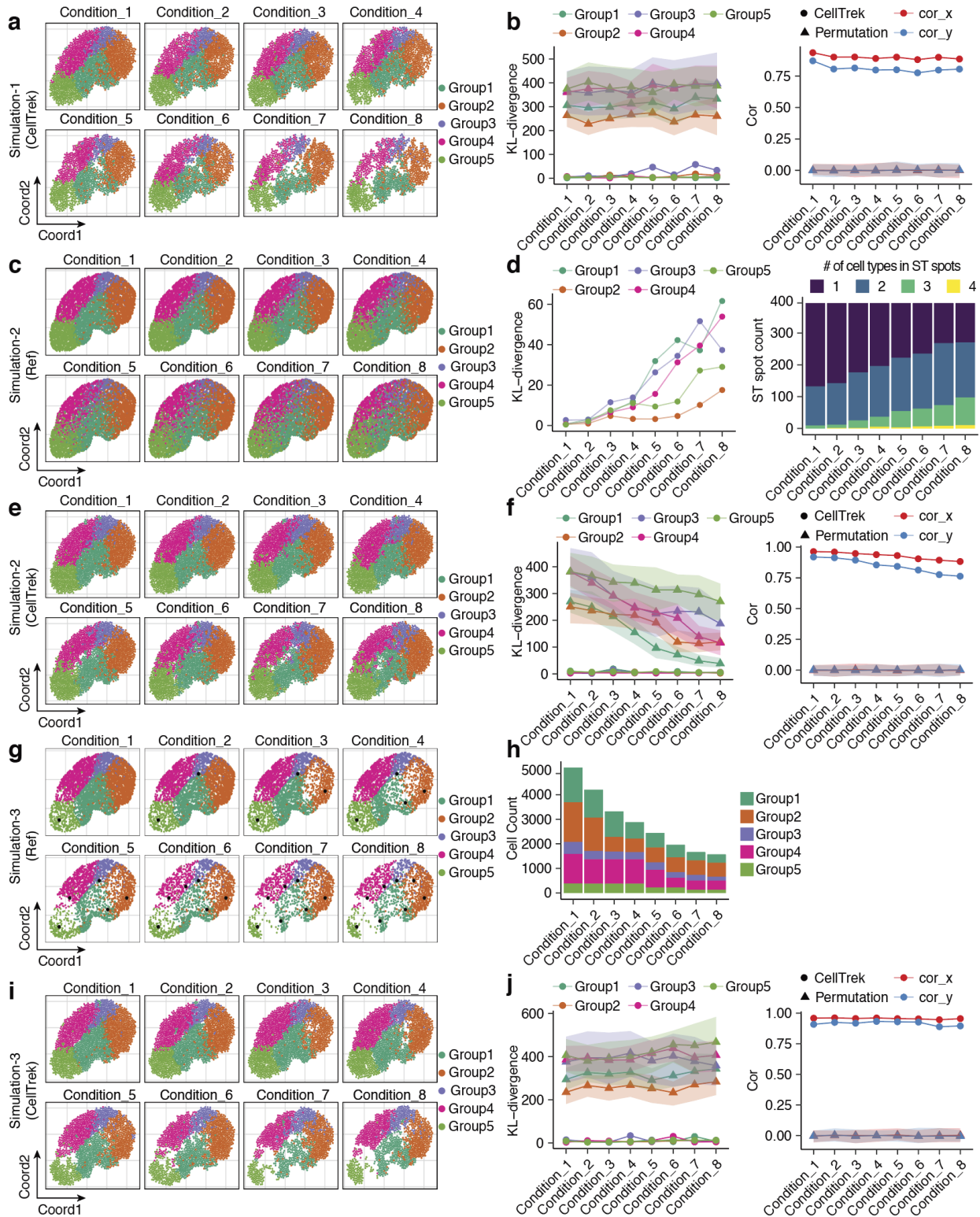
Supplementary Figure 2 – Three spatial single-cell datasets for benchmarking

(a) UMAP of a simulated scRNA-seq data with 5 cell groups. (b) Spatial organization of the simulated data as the ground truth. (c) ST data generated based on panel (b). (d) UMAP of *Drosophila* embryo FISH-generated single cell data. (e) Spatial organization of *Drosophila* embryo cells as the ground truth. (f) *Drosophila* embryo ST data generated based on panel (e). (g) UMAP of mouse embryo seqFISH data (Group1: Cardiomyocytes; Group2: Cranial mesoderm; Group3: Definitive endoderm; Group4: Dermomyotome; Group5: Endothelium; Group6: Erythroid; Group7: Forebrain midbrain hindbrain; Group8: Gut tube; Group9: Haematoendothelial progenitors; Group10: Intermediate mesoderm; Group11: Lateral plate mesoderm; Group12: Mixed mesenchymal mesoderm; Group13: Neural crest; Group14: Presomitic mesoderm; Group15: Spinal cord; Group16: Splanchnic mesoderm; Group17: Surface ectoderm). (h) Spatial organization of the mouse embryo cells as the ground truth. (i) mouse embryo ST data generated based on panel (h). In (c), (f) and (i), each ST spot aggregates the 5 nearest cells to generate the ST data.



Supplementary Figure 3 – Benchmarking on three datasets with known spatial references

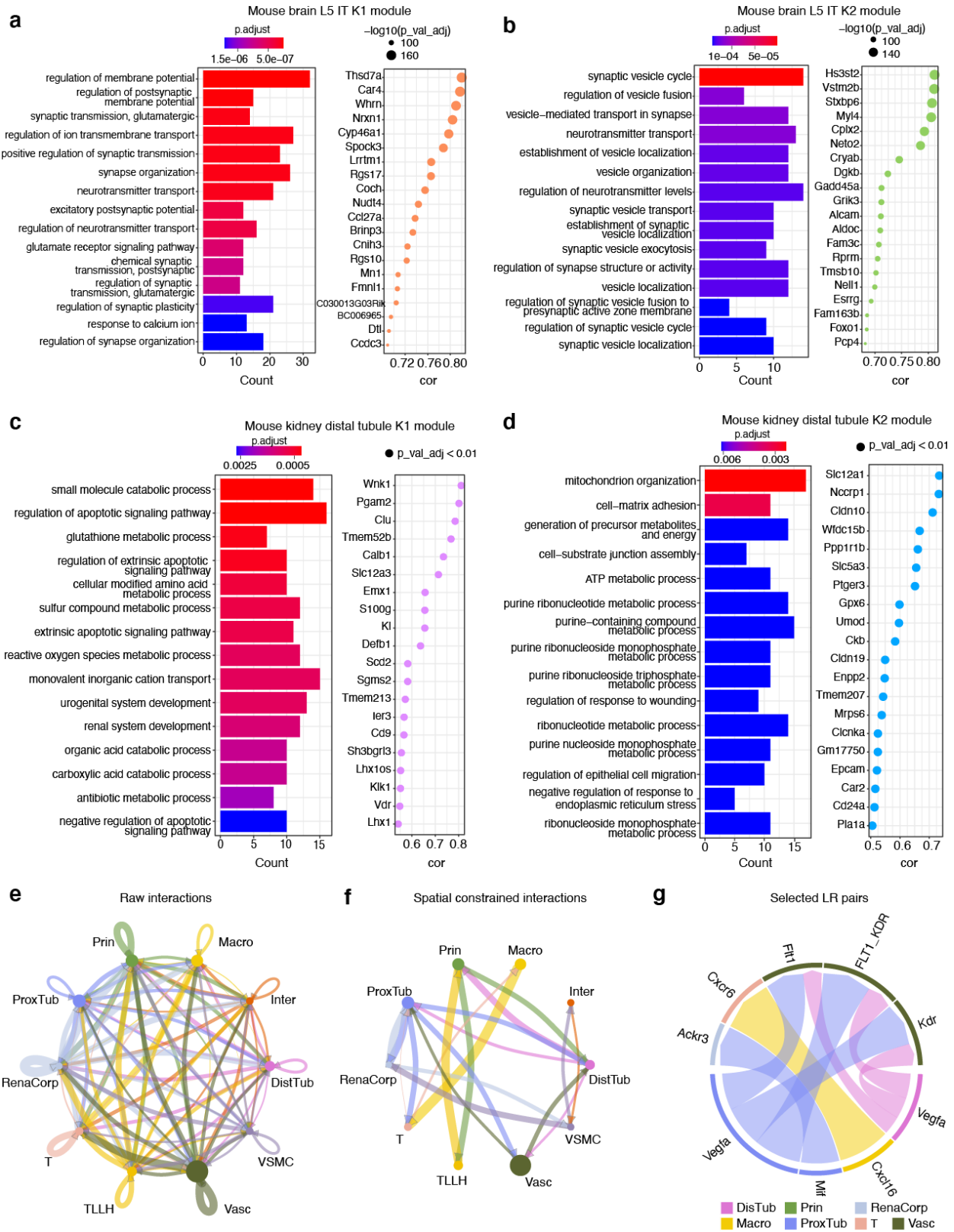
(a) Comparison of the ground-truth reference, CellTrek, NVSP-CellTrek and SrtCT results on the simulated data. (b) KL-divergence of spatial cell charting methods for each cell type compared with the ground-truth. (c) Comparison of the ground-truth reference, CellTrek, NVSP-CellTrek and SrtCT results on the *Drosophila* embryo data. (d) KL-divergence of spatial cell charting methods for each cell type compared with the ground-truth. (e) The expression of *Drosophila* embryogenic marker genes (*eve*, *hb*, *ken*, *Kr* and *sna*) on the CellTrek map. (f) Comparison of the ground-truth reference, CellTrek, NVSP-CellTrek and SrtCT results on the mouse embryo data. (g) KL-divergence of three spatial cell charting methods for each cell type compared with the ground-truth. (h) The CellTrek map of a subgroup of gut tube (foregut cells) and the marker genes (*Foxa1* and *Cldn4*). (i) Trajectory analysis for foregut tube cells (left) and CellTrek spatial mapping of the pseudotime values in the tissue section (right).



Supplementary Figure 4 – Simulation study of CellTrek under different data conditions

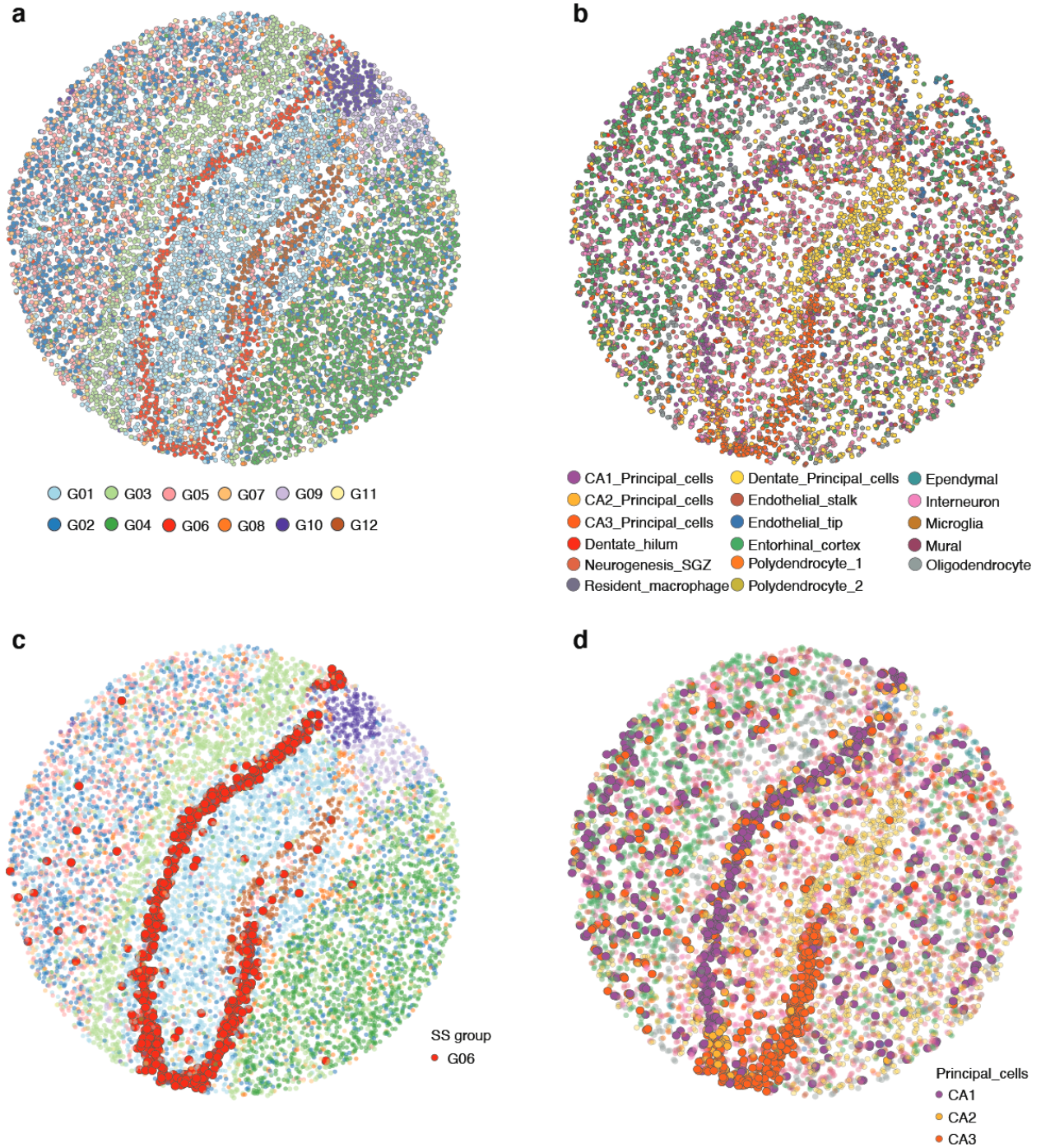
(a) CellTrek results under different gene counts in the simulated data. From condition 1 to condition 8, the gene counts decreased. (b) KL-divergence (left) and spatial coordinate

correlation (right) of CellTrek and permutation test across different gene count conditions. **(c)** Simulation of the increasing spatial randomness of the reference data from condition1 to condition8. **(d)** KL-divergence of the simulated reference compared with the raw spatial cell organization (left) and the number of cell types in ST spot (right) across different spatial randomness conditions. **(e)** CellTrek results under different spatial randomness of the reference data. **(f)** KL-divergence (left) and spatial coordinate correlation (right) of CellTrek and permutation test across different spatial randomness conditions. **(g)** Simulation of the decreasing tissue spatial densities (cell numbers) of the reference data from condition1 to condition8. Black dots display the marker points for spatial down-sampling. **(h)** Bar plot showing the number of cells under different tissue spatial density conditions. **(i)** CellTrek results under different tissue densities of the reference data. **(j)** KL-divergence (left) and spatial coordinate correlation (right) of CellTrek and permutation test across different tissue spatial density conditions. Detailed parameter settings are provided in Supplementary Table 1-3. For the permutation tests, the ribbon shows the 95% confidence intervals.



Supplementary Figure 5 – Mouse brain and kidney co-expression module enrichment analysis and mouse kidney spatial constrained cell-cell interaction analysis

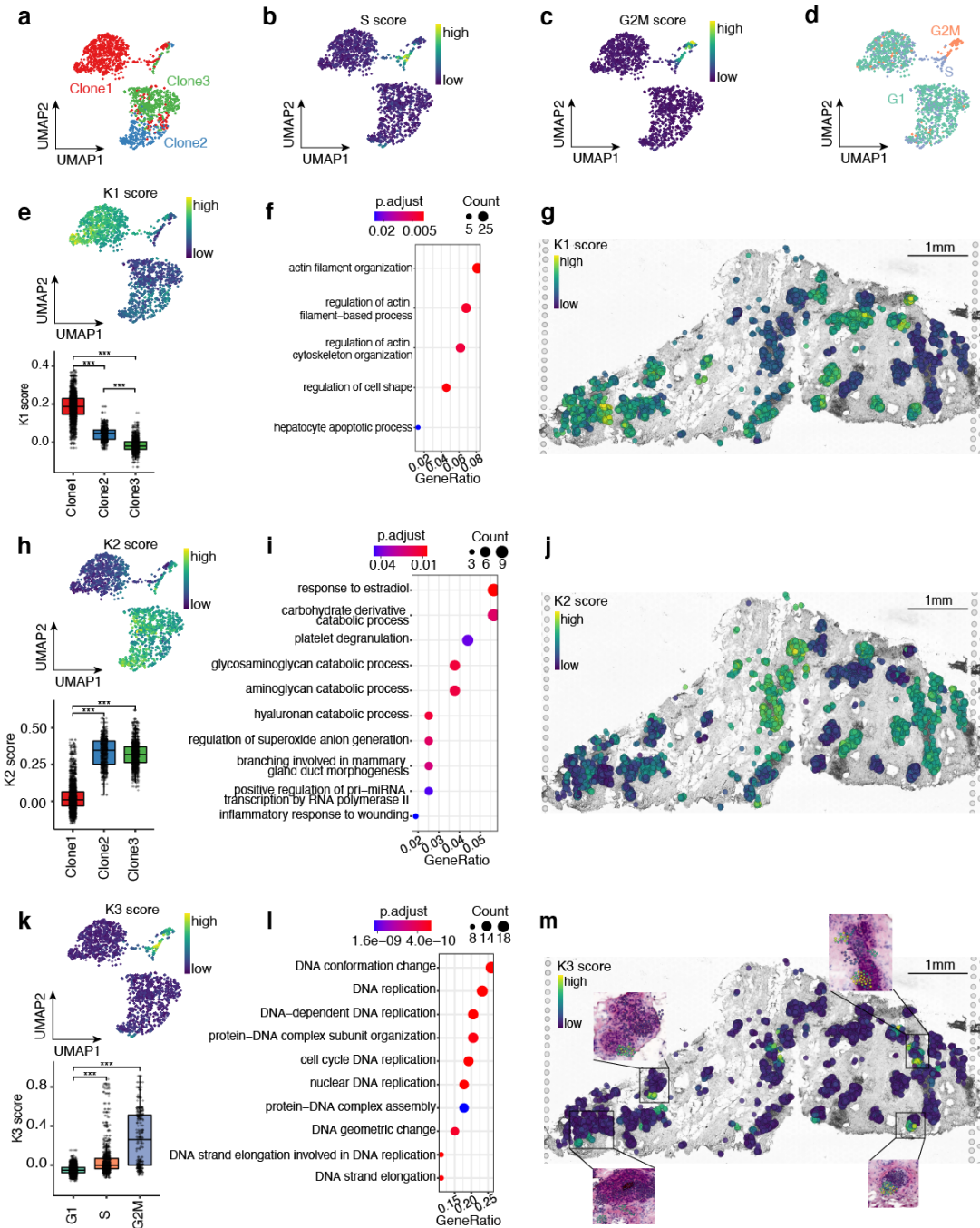
(a-b) GO enrichment analyses (left) and module-correlated genes (right) for mouse brain L5 IT K1 and K2 modules, respectively. (c-d) GO enrichment analyses (left) and module-correlated genes (right) for mouse kidney distal tubule K1 and K2 modules, respectively. (e) Summary of cell-cell interaction network of mouse kidney cells using CellChat. (f) Spatial constrained cell-cell interaction network of mouse kidney cells. (g) Chord plot showing some identified ligand-receptor pairs. The edge width in (e) and (f) represent the total interaction strength; and the arc width in (g) represent the interaction score calculated from CellChat. The direction of the arrows goes from the ligands to the receptors. In a-d, P values were calculated by hypergeometric distribution and adjusted by Benjamini-Hochberg method. Module-correlated genes were determined by the CellTrek *FindCorMarkers* module. Spearman correlation was performed and P values were adjusted by the Bonferroni method.



Supplementary Figure 6 – CellTrek analysis of mouse hippocampus Slide-seq data
(a) Unsupervised clustering of mouse hippocampus Slide-seq data identified 12 clusters. **(b)** CellTrek spatial mapping of scRNA-seq data to the tissue section. **(c)** Slide-seq data with G06 group highlighted. **(d)** CellTrek map with three principal cells (CA1, CA2 and CA3) highlighted which corresponded to G06.

Supplementary Figure 7 – ScRNA-seq and ST analyses of DCIS1

(a) UMAP of DCIS1 scRNA-seq data. (b) Consensus heatmap of scRNA-seq data for top differentially expressed genes for each cell type. (c) CellTrek result of three tumor subclones (clone1-3) which is also presented in **Fig. 4e**. (d) Unsupervised clustering of ST tumor spots identified five clusters (ST1-5). (e) Gene expression-based Spearman correlation analysis between three tumor subclones in the scRNA-seq data (clone1-3) and five ST clusters (ST1-5).



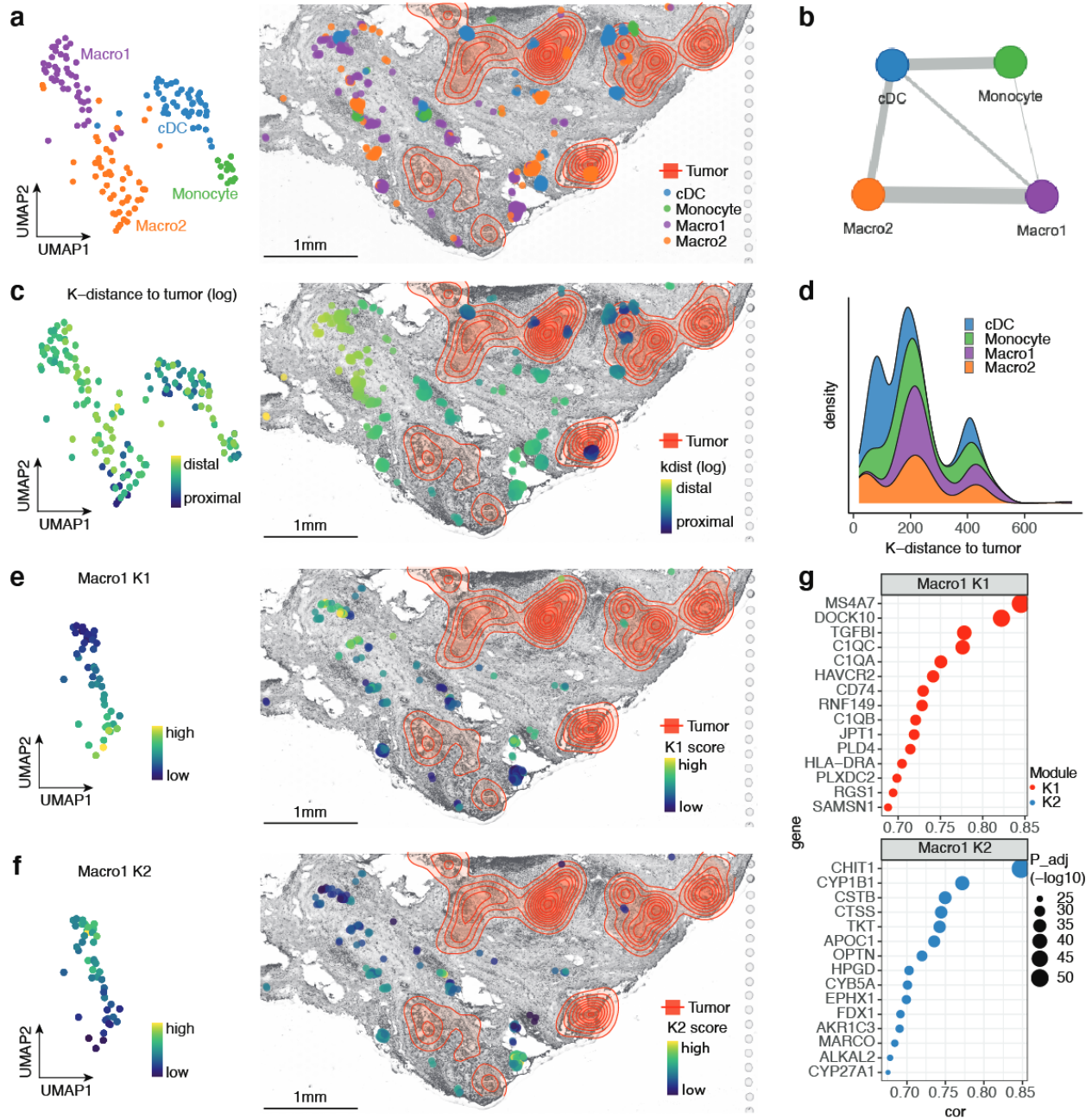
Supplementary Figure 8 – Spatial co-expression patterns of tumor cells in DCIS1

(a) Transcriptome-based UMAP of three tumor subclones identified from DCIS1 scRNA-seq data (Clone1 n = 1,295; Clone2 n = 523; Clone3 n = 862). Seurat-based cell cycle analysis on tumor cells showed S scores (b), G2M scores (c) and categorical cell cycle phases (G1 n = 2,060; G2M n = 508; S n = 1,019) (d). (e) K1 module scores on the UMAP (upper) and boxplot across tumor subclones (lower). (f) GO enrichment analysis for the K1 module. (g) CellTrek map of K1 module scores. (h) K2 module scores on the UMAP (upper) and boxplot across tumor subclones (lower). (i) GO enrichment analysis for the K2 module. (j) CellTrek map of K2 module scores. (k) K3 module scores on the UMAP (upper) and boxplot across different cell cycle phases (lower). (l) GO enrichment analysis for the K3 module. (m) CellTrek map of K3

module scores. In e, h, and k two-sided Wilcoxon rank-sum tests were performed. Boxplots show the median with interquartile ranges (25–75%); whiskers extend to 1.5X the interquartile range from the box. In **f**, **i** and **l**, *P* values were calculated by hypergeometric distribution and further adjusted by Benjamini-Hochberg method.

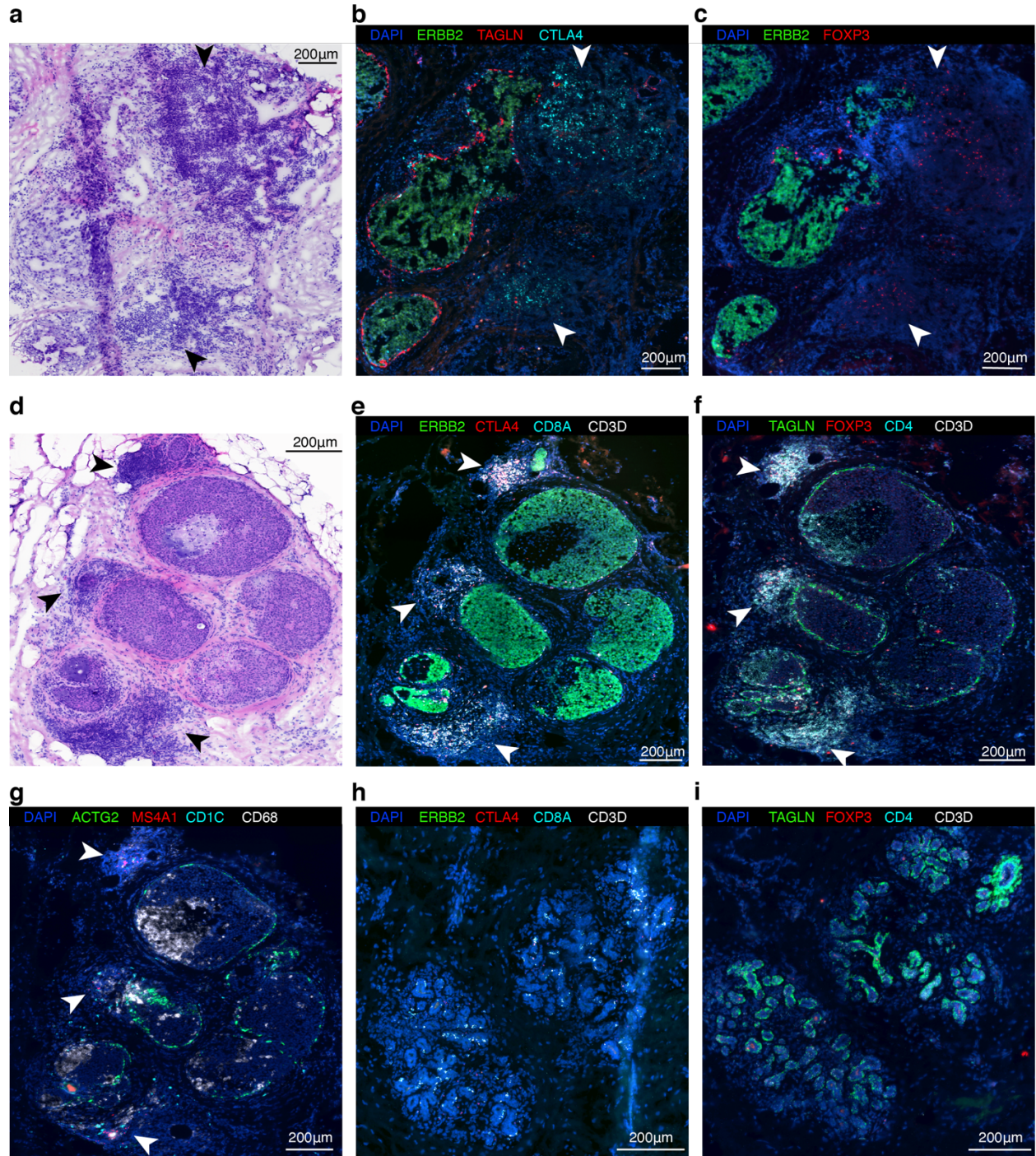
Supplementary Figure 9 – ScRNA-seq data analysis of DCIS2

(a) UMAP of DCIS2 scRNA-seq data, with clusters corresponding to different cell types. (b) Consensus heatmap of top differentially expressed genes for each cell cluster. (c) Heatmap of CopyKAT inferred copy number profiles from the scRNA-seq data and hierarchical clustering of cells. (d) Violin plots showing expression of canonical T cell state markers across different T cell states. (e) Consensus heatmap showing expression of top differentially expressed genes across different myeloid cell states.



Supplementary Figure 10 – CellTrek analyses of myeloid cell states in DCIS2

(a) UMAP representation of myeloid cell states (left) and corresponding CellTrek map (right) (b) Spatial graph of myeloid cell states colocalization using SCOLoc. (c) UMAP (left) and CellTrek map (right) of myeloid cells K-distance to tumor cells. (d) Density plot of K-distances to tumor cells for each myeloid cell state. (e) UMAP (left) and CellTrek map (right) of Macro1 K1 module scores. (f) UMAP (left) and CellTrek map (right) of Macro1 K2 module scores. (g) Macro1 K1 (top) and K2 (bottom) module top correlated genes. The contour plots represent the densities of tumor cells. Module-correlated genes were determined by the CellTrek *FindCorMarkers* module. Spearman correlation was performed and P values were adjusted by the Bonferroni method.



Supplementary Figure 11 – Orthogonal validation of tumor and immune cell spatial distributions using RNAscope assay in DCIS2 and DCIS3

(a) H&E image of the DCIS2 tumor region. (b) RNAscope assay for *ERBB2*, *TAGLN* and *CTLA4* in DCIS2 tumor region. (c) RNAscope assay for *ERBB2* and *FOXP3* in DCIS2 tumor region. Data in (a-c) were collected from adjacent tissue slides. (d) H&E image of the DCIS3 tumor region. (e) RNAscope assay for *ERBB2*, *CTLA4*, *CD8A* and *CD3D* in DCIS3 tumor region. (f) RNAscope assay for *TAGLN*, *FOXP3*, *CD4* and *CD3D* in DCIS3 tumor region. (g) RNAscope assay for *ACTG2*, *MS4A1*, *CD1C* and *CD68* in DCIS3 tumor region. (h) RNAscope assay for *ERBB2*, *CTLA4*, *CD8A* and *CD3D* in DCIS3 adjacent normal lobular region. (i) RNAscope assay for *TAGLN*, *FOXP3*, *CD4* and *CD3D* in DCIS3 adjacent normal lobular region. Arrows point to different immune cell markers near the DCIS tumor ducts.

Supplementary Tables

Supplementary Table 1 Parameter settings for different conditions in simulation-1

Condition	scRNA-seq				ST			
	Counts	Cell Proportion	Median Count	Median Gene	Counts	Spot Proportion	Median Count	Median Gene
1	10	0.2	2815	494	50	0.2	15732	1526
2	10	0.4	2328	414	50	0.4	12516	1356
3	15	0.4	2195	414	75	0.4	12489	1356
4	15	0.5	1781	207	75	0.5	7006	338
5	20	0.5	1622	192.5	100	0.5	5055	320
6	20	0.6	929	63	100	0.6	2257	39
7	25	0.6	671	42	125	0.6	1537	23
8	25	0.7	444.5	31	125	0.7	1183	19

Counts means the UMI counts for each gene we downsampled and Cell/Spot Proportion means the proportion of cells/ST spots were used for downsampling. Median Count and Gene mean the median of UMI count and gene number after downsampling.

Supplementary Table 2 Parameter settings for different conditions in simulation-2

Condition	Spatial Deviation
1	30
2	60
3	90
4	120
5	150
6	180
7	210
8	240

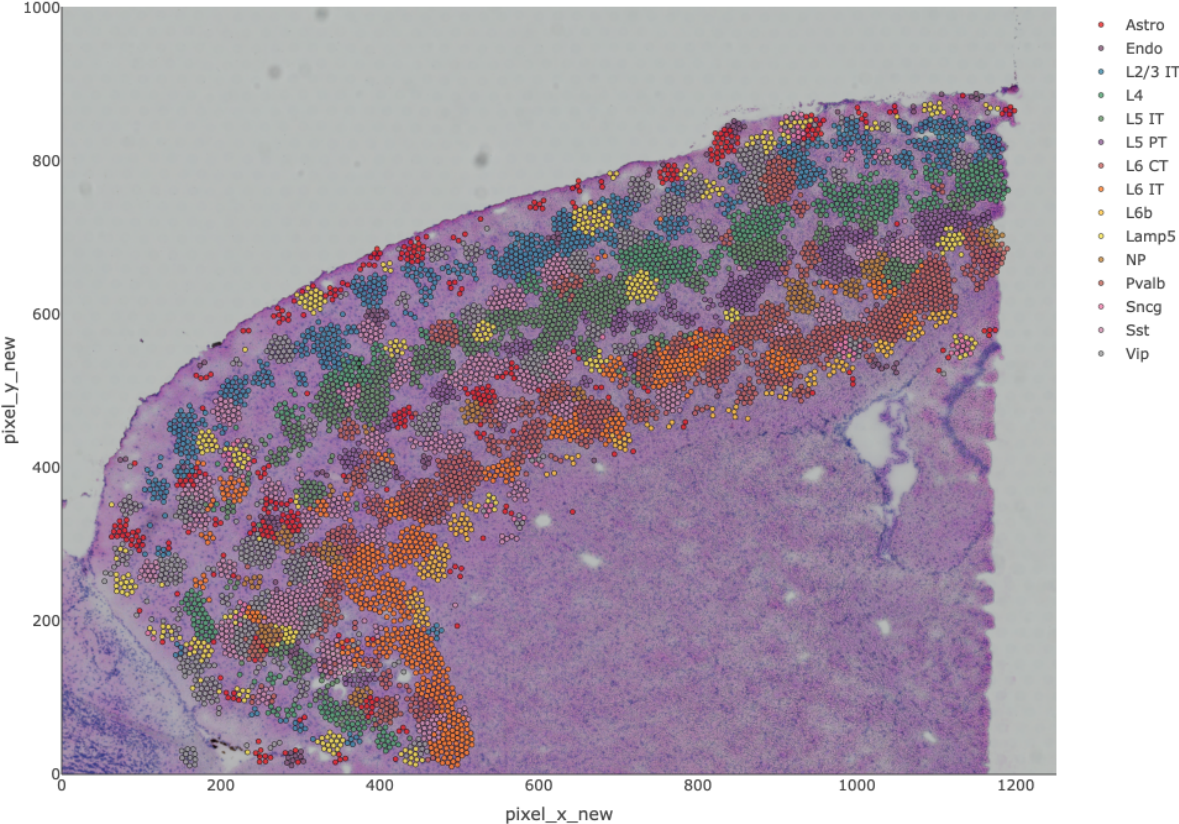
Spatial Deviation means the deviation of the spatial gaussian noise we added to the cell.

Supplementary Table 3 Parameter settings for different marker points in simulation-3

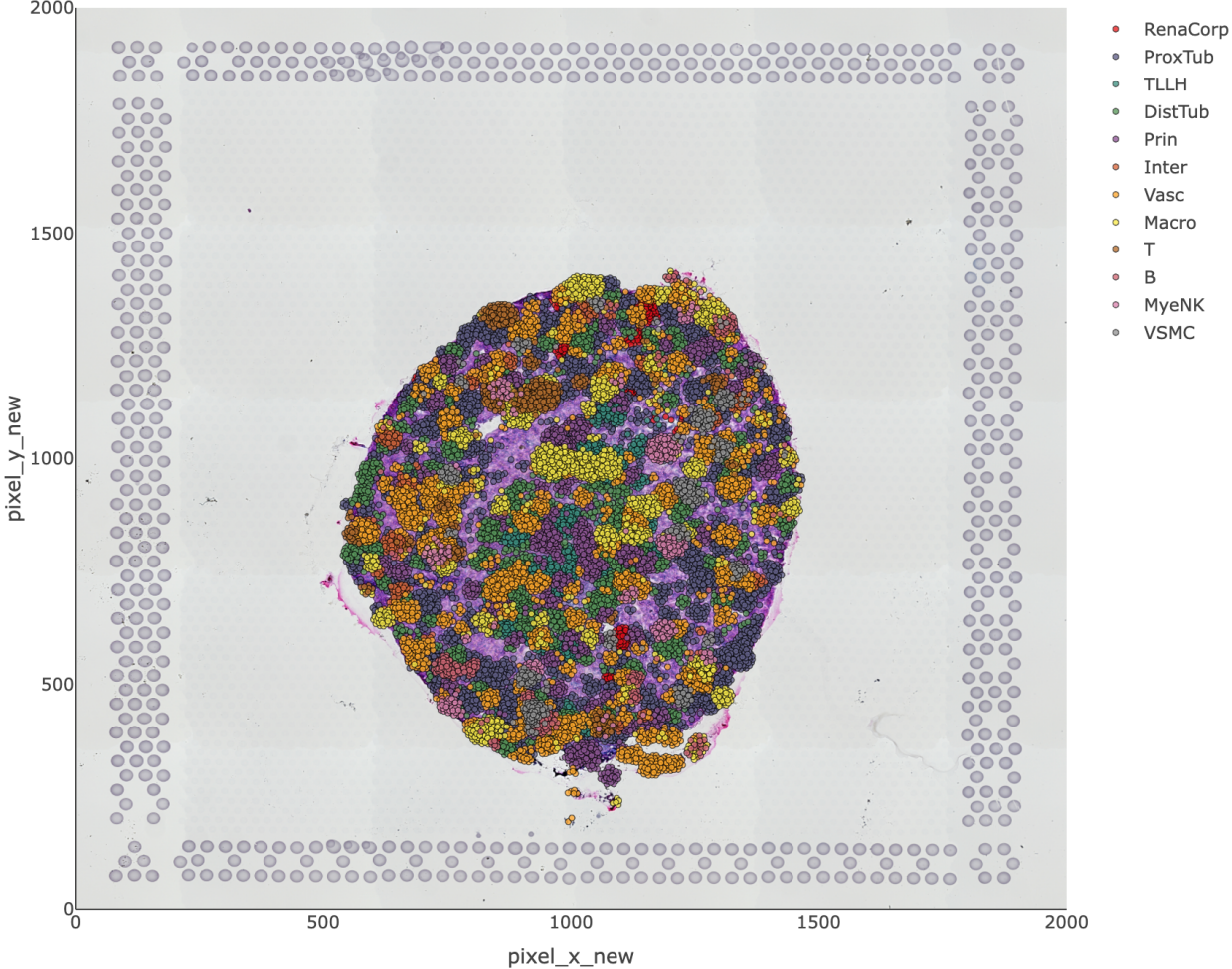
MarkerPoint	X-coordinate	Y-coordinate
1	350	300
2	1300	1100
3	1950	800
4	1500	600
5	600	800
6	1000	1000
7	900	400
8	1700	1100

Supplementary Data

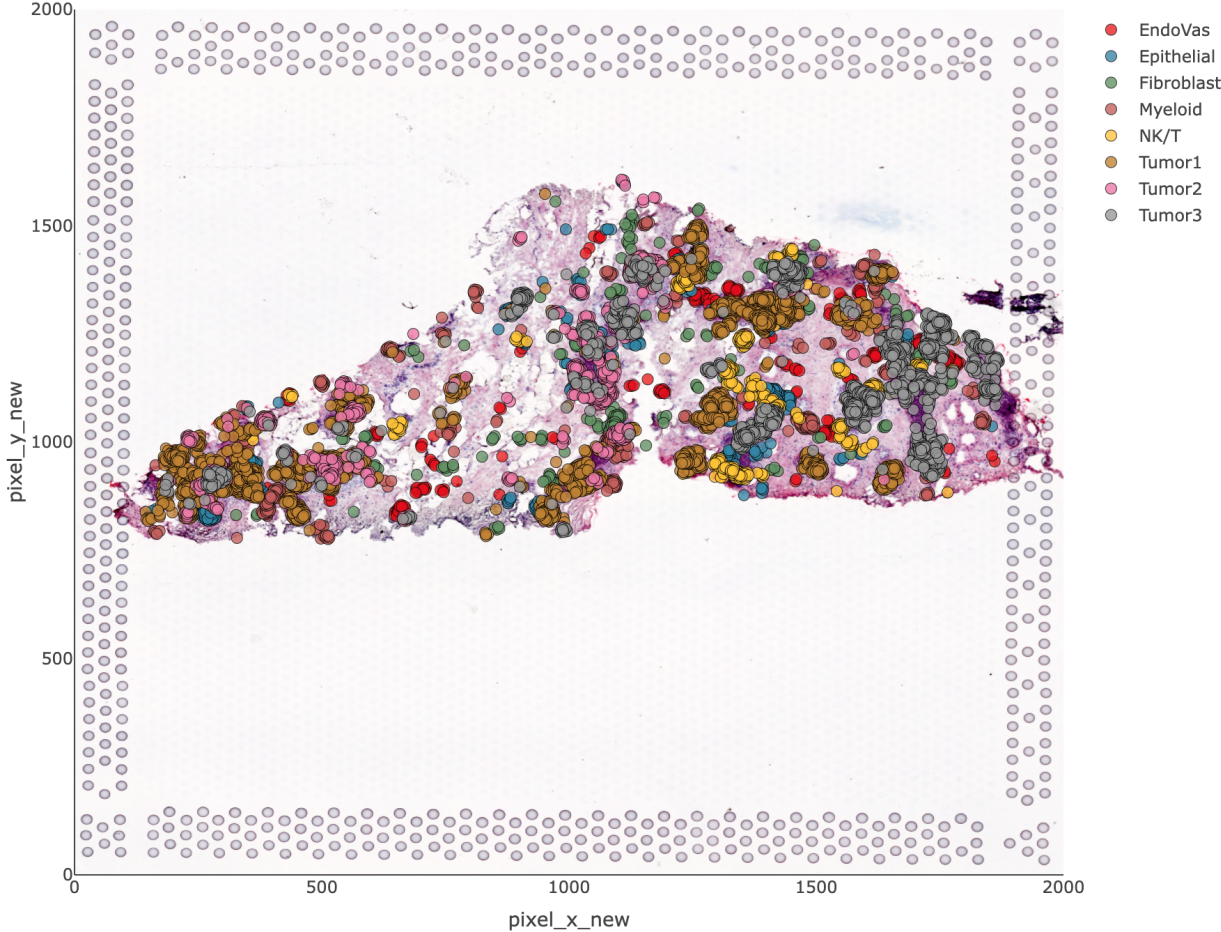
Supplementary Data 1 – Screenshot of the CellTrek result for mouse brain data



Supplementary Data 2 – Screenshot of the CellTrek result for mouse kidney data



Supplementary Data 3 – Screenshot of the CellTrek result for DCIS1 data



Supplementary Data 4 – Screenshot of the CellTrek result for DCIS2 data

